DOE/SC-ARM-TR-317

Three-Channel Sunphotometer Cloud Mode Value-Added Product Report

LL Ma
JD Rausch
C Chiu
SE Giangrande
D Wang

June 2025

DISCLAIMER

Three-Channel Sunphotometer Cloud Mode Value-Added Product Report

LL Ma, Brookhaven National Laboratory (BNL)
SE Giangrande, BNL
JD Rausch, BNL
D Wang, BNL
C Chiu, Colorado State University

June 2025

How to cite this document:

Ma, LL, SE Giangrande, JD Rausch, D Wang, and C Chiu. Three-Channel Sunphotometer Cloud Mode Value-Added Product Report. U.S. Department of Energy, Atmospheric Radiation Measurement user facility, Richland, Washington. DOE/SC-ARM-TR-317.

Work supported by the U.S. Department of Energy,
Office of Science, Office of Biological and Environmental Research

Acronyms and Abbreviations

AERONET	Aerosol Robotic Network
ARM	Atmospheric Radiation Measurement
ASCII	American Standard Code for Information Interchange
CSPHOT	Cimel sunphotometer
DISORT	discrete-ordinate-method radiative transfer
DOE	U.S. Department of Energy
ENA	Eastern North Atlantic
EPC	Eastern Pacific Cloud Aerosol Precipitation Experiment (EPCAPE)
ESM	Earth system model
FOV	field of view
GUC	Surface Atmosphere Integrated Field Laboratory (SAIL), near Gunnison, Colorado
KAZR	Ka ARM Zenith Radar
LUT	look-up table
LWP	liquid water path
MFRSR	multifilter rotating shadowband radiometer
MICROBASE	Continuous Baseline Microphysical Retrieval Value-Added Product
MODIS	Moderate Resolution Imaging Spectroradiometer
MWRRET	Microwave Radiometer Retrievals Value-Added Product
NASA	National Aeronautics and Space Administration
NetCDF	Network Common Data Form
Sc	stratocumulus cloud
SGP	Southern Great Plains
TROPoe	Tropospheric Optimal Estimation Retrieval Value-Added Product
VAP	value-added product

Contents

Figures

Tables

1.0 Introduction

A primary source of uncertainty in Earth system model (ESM) predictions is the representation of cloud processes and associated cloud feedback. Several fundamental cloud properties critical to the understanding of aerosol-cloud interactions are poorly constrained by observations, with key deficiencies in our observations of cloud and precipitation droplet sizes and cloud optical depth. Observations of these cloud properties are often challenging to estimate from remote-sensing platforms and costly to obtain from in situ aircraft. Nevertheless, observations of boundary-layer clouds, and improved knowledge of stratocumulus cloud (Sc) processes, are especially important to ESM advancement. This is because these clouds have extensive coverage and exert controls on boundary-layer dynamics and the global radiative energy balance.

One emphasis for the ARM facility is to provide information on cloud properties for process studies, including insights on the cloud droplet effective radius, r_e, cloud optical depth, τ, and/or liquid water path (LWP). One such capable instrument is a multispectral photometer. The U.S. Department of Energy (DOE) Atmospheric Radiation Measurement (ARM) user facility has deployed photometers at its fixed and mobile facility deployments for over two decades. As a narrow-field-of-view (FOV, 1.2°) instrument, one advantage of this instrument is in its viability for sampling a range of broken to overcast cloud cover conditions. Originally designed to retrieve aerosol optical properties, it was suggested by Marshak et al. (2004) and later expanded by Chiu et al. (2006, 2010, 2012) that the National Aeronautics and Space Administration (NASA) AERosol RObotic NETwork (AERONET; Holben et al. 1998) implement a "cloud mode" strategy for its multispectral photometers (Sun-Sky-Lunar Multispectral Photometer). This mode is performed using two-channel radiance measurements during instrument sequences where clouds completely block the sun. When operated in this fashion, the mode enables estimates of the cloud optical depth (τ). Recently, ARM upgraded its photometers to a three-channel (440, 870, and 1640-nm wavelength) configuration to further constrain retrievals that simultaneously capture τ and cloud particle effective radius (Chiu et al. 2012). While previous two-channel (440, 870-nm) methods were applicable over vegetated land surfaces, this third channel constraint enables retrievals over ocean and ice surfaces, suitable for a range of higher-latitude and shipborne deployments.

ARM has deployed sunphotometers to its fixed observatories such as the Southern Great Plains (SGP) and the Eastern North Atlantic (ENA), as well as its mobile facilities on request for field campaigns (e.g., Mather and Voyles 2013, Wood et al. 2015, Wang et al. 2022). This ARM value-added product (VAP) draws on the extended ARM measurement record with a goal to deliver photometer-retrieved quantities of cloud properties as a baseline, continuing operational product. The VAP currently is developed targeting several sunphotometer cloud retrieval quantities – the cloud optical depth and the cloud droplet effective radius. This VAP also estimates the liquid water path from those two retrieved quantities. A summary of VAP performance for an extended SGP and ENA Sc data set – including uncertainty estimates and comparisons with collocated ARM sensors – is also available in Sookdar et al. (2025).

2.0 Algorithm Outline

Chiu et al. (2012) developed a three-channel sunphotometer retrieval algorithm (using wavelengths of 440, 870, and 1640 nm) and outlined the motivation behind its creation. Chiu et al. (2012) also provided a detailed explanation of the retrieval process on which this ARM VAP is based. Recently, Sookdar et al. (2025) also documented the operational ARM VAP algorithm and its performance as well as uncertainty considerations for extended Sc studies at ARM sites.

The Cimel sunphotometer is a ground-based scanning photometer for passive remote sensing of the atmosphere, with NASA AERONET calibrating and maintaining these instruments, while processing certain data as part of their global archive. During its “cloud mode”, the instrument points to zenith and obtains high-gain, sky-mode observations of radiance in at least six of its nine channels: 380 (newer CE318T models), 440, 500, 675, 870, 1020, and 1640-nm wavelengths. Although the instrument requires less than five minutes to cycle through these channels, the availability for scheduling “cloud mode” retrievals is limited by the overall photometer sequencing and contingent on the solar zenith angle and instrument model. For much of the ARM data record, VAP retrievals can be performed at 15-minute intervals (i.e., prior to October 2017 at SGP, February 2021 at ENA) when environmental conditions allowed. New models improve the availability to five-minute updates when not operating in any of the other observing modes.

The automated retrievals we implement use zenith radiance measurements at 440, 870, and 1640-nm wavelengths. This approach simultaneously retrieves τ and r_e, with these quantities used to compute LWP in g·m^{-2} as:

$$\mathrm{LWP} = \frac{2}{3}\rho_w \tau\, r_e \tag{1}$$

where ρ_w is the density of water, 10^6 g·m^{-3}, r_e is in meters, τ is unitless, and the expression in (1) assumes that liquid water content is constant in the vertical (Stephens 1978). The inputs to the algorithm are the calibrated photometer zenith radiance measurements and surface albedo estimated from the Terra and Aqua Moderate Resolution Imaging Spectroradiometer (MODIS, "MCD43A2 and “MCD43A3" products, e.g., Schaaf et al. 2002).

The ground-based zenith radiance for clouds at a given wavelength may be expressed as functions of the incoming radiance, the cloud r_e and τ, and the albedo of the underlying surface. By including the 1640-nm water-absorbing wavelength, Chiu et al. (2012) three-channel constraint methods enabled r_e estimates since the zenith radiance behavior for 1640 nm decreases with droplet size due to absorption, whereas radiances at 870 nm increase due to forward scattering. In practice, retrieval sensitivity of zenith radiance measurements to larger droplet size, as well as other practical limitations for radiance and surface albedo estimates, may undermine the usefulness of this third channel for r_e retrievals. To mitigate the diminishing nature of those effects, Chiu et al. (2012) implemented a multi-step perturbation approach to assess retrieval uncertainty. This approach first considers a 5-10% uncertainty (normally distributed, input sensitivity) in zenith radiance and surface albedo measurements. The perturbed zenith radiances are subsequently compared to a calculated look-up table computed from the discrete-ordinate-method radiative transfer model (DISORT; Stamnes et al. 1988) over input ranges typical for ARM sites.

This implementation follows Chiu et al. (2012) by defining a solution from the photometer retrieval as "viable" when the zenith radiances agree with the look-up table to within 10% at the 440 and 870-nm wavelengths. Any viable solutions are sorted based on errors in the zenith radiance at the 1640 nm, with the five best solutions (i.e., smallest errors) averaged to generate a single solution for the set of the perturbed zenith radiance and surface albedos. Chiu et al. (2012) recommended this procedure be repeated 40 times using randomly generated perturbations. Reported retrievals for τ and r_e are obtained by taking the mean of 40 repetitions. Sensitivity tests (not shown) that considered additional perturbations did not produce significant changes in the retrieved quantities.

This perturbation uncertainty (defined here as calculating the standard error) is reported by these photometer retrievals as its instantaneous retrieval uncertainty. In Sookdar et al. (2025), the average values for these reported uncertainties at ENA in τ and r_e estimates are 1.19 (unitless) and 2.1 µm, respectively. For the SGP, they estimated these uncertainties as 1.56 (unitless) for τ and 1.46 µm for r_e. These values may also be reported as relative errors at a level of 5-10% of the reported τ estimates, or 15-20% of the reported r_e estimates. An example for the τ outputs from SPHOT and MFRSR, along with corresponding ARM KAZR radar fields, is shown in Figure 1.

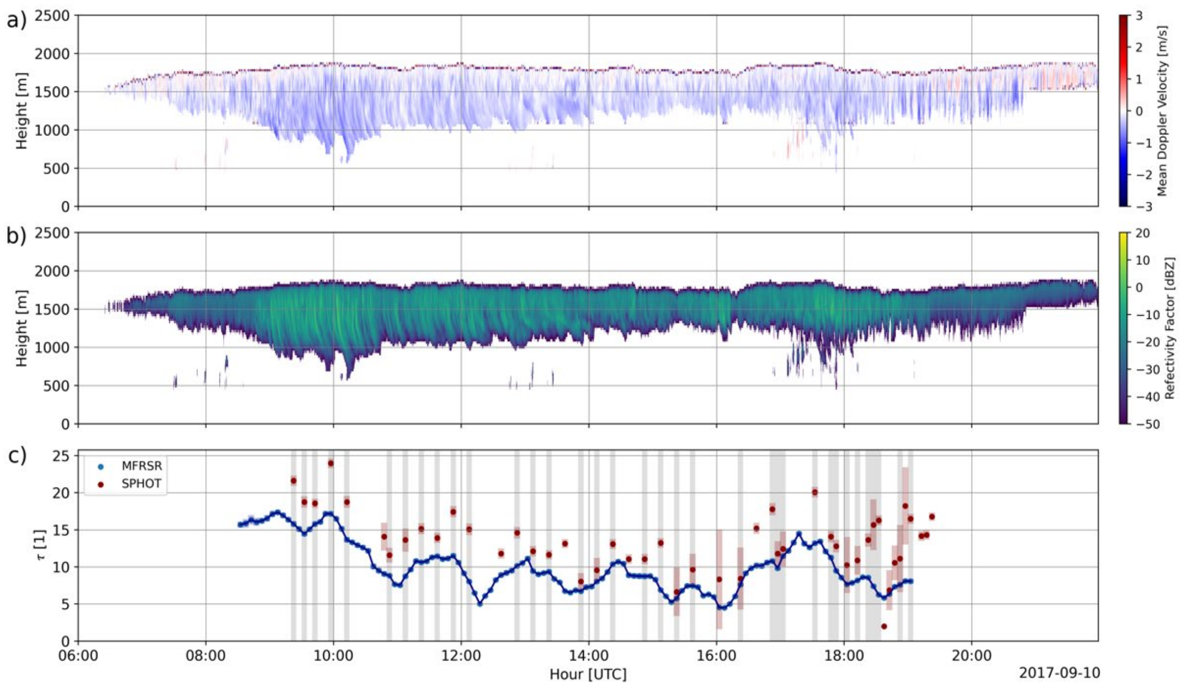

Figure 1. The Ka ARM Zenith Radar (KAZR) (a) mean Doppler velocity and (b) radar reflectivity factor for the 10 September 2017 event at ENA. (c) Cloud optical depth, τ, retrievals from the SPHOT (red) and MFRSR (blue), with shaded (grey) regions indicating cloud samples used in comparisons for this study.

3.0 Input Data

The cloud mode VAP uses the following datastreams as inputs:

MODIS Albedo: modisalbedo.00/ modisalbedoqc.00

Extracted from the MODIS "MCD43A2 and “MCD43A3" combined Terra and Aqua data product, this data is captured at a 500-m spatial resolution over a 16-day period. The MODIS albedos are computed daily for the ninth day within a 16-day window of cloud-free scene retrievals.

Pre-calibrated Zenith Radiances from AERONET: csphotzenradv3.a1

Data for the three channels (440, 870, and 1640 nm) is obtained from AERONET. These radiances are initially in ASCII format but are converted to a NetCDF file format, which is accessible through ARM Data Discovery.

Solar Constant: sslrcnst

The solar constant values for each instrument deployed at the sites are sourced from AERONET. This information is provided in ASCII format.

Look-up Table: LUT.I0 (Id, Rd and T0).wavelength

Using an atmosphere radiative transfer model, the VAP employs a look-up table for efficient retrieval and analysis of relevant data.

The detailed variable descriptions are provided in Table 1-3, Appendix A.

4.0 Output Datastream

The name of the output file is: **###sphotcod2chiuF#.c1.YYYYMMDD.hhmmss.nc**

Where: ### the site of the instrument location
F#: facility ID
YYYY year, MM - month of the year, DD - day of the month, hh - hour of the day, mm - minute of the hour, ss - second of the minute of data start.

The output NetCDF files from the Cloud-Optical-Depth VAP adhere to the ARM data standards. These files encompass the computed values of cloud optical depth, effective radius, and liquid water path, along with their associated uncertainties.

The detailed variable descriptions are provided in Table 4, Appendix B.

5.0 Sites Where the SPHOCOD VAP Is Expected to Run

The Cloud-Optical-Depth Value-Added-Product (VAP) will undergo processing for all permanent ARM sites and AMF deployment locations, including SGP/C1, ENA/C1, EPC/M1 (Eastern Pacific Cloud Aerosol Precipitation Experiment [EPCAPE] in La Jolla, California) , GUC/M1, (Surface Atmosphere Integrated Field Laboratory [SAIL] near Gunnison, Colorado), etc. However, it is important to acknowledge that in the initial dates, the intentional deactivation of cloud mode during the winter and early spring limited the availability of data. As a result, the earlier VAP data prior to 2017 will only be accessible from early March to October.

6.0 Validation Efforts

As mentioned, an accompanying validation effort for this VAP was performed by Sookdar et al. (2025) for Sc conditions at the ENA and SGP sites. Overall, they reported modest agreement in key quantity retrievals between routine sunphotometer VAP outputs and collocated ARM profiling references. A correlation of ≅ 0.81 is found between photometer τ retrievals and those from the shadowband radiometer measurements, with photometer retrievals reporting a high (relative) bias. The τ intercomparisons indicated that variability between ARM retrievals can be as high as a factor of three larger than the errors reported from individual retrieval input perturbation tests. Photometer r_e retrievals for this VAP suggested low correlations (< 0.1) having a standard deviation ≅ 3 mm when compared to ARM baseline multi-sensor radar/radiometer references (i.e., those from ARM's Continuous Baseline Microphysical Retrieval [MICROBASE] VAP). However, photometer LWP calculations from this VAP remain relatively unbiased in non-drizzling conditions, with errors of the order of [50 g m^{-2}] and correlations ≅ 0.7 to collocated radiometer and interferometer references (e.g., ARM's Microwave Radiometer Retrievals [MWRRET] or Tropospheric Optimal Estimation Retrieval [TROPoe] VAPs). Users are encouraged to consult that manuscript for further details on their event selection and error characterization.

7.0 References

AEronet: http://aeronet.gsfc.nasa.gov/

Chiu, JC, A Marshak, Y Knyazikhin, W Wiscombe, H Barker, JC Barnard, and Y Luo. 2006. "Remote sensing of cloud properties using ground-based measurements of zenith radiance." *Journal of Geophysical Research – Atmospheres* 111(D16): D16201, https://doi.org/10.1029/2005JD006843

Chiu, JC, C-H Huang, A Marshak, I Slutsker, DM Giles, BN Holben, Y Knyazikhin, and WJ Wiscombe. 2010. "Cloud optical depth retrievals from the Aerosol Robotic Network (AERONET) cloud mode observations." *Journal of Geophysical Research – Atmospheres* 115(D14): D14202, https://doi.org/10.1029/2009JD013121

Chiu, JC, A Marshak, C-H Huang, T Várnai, RJ Hogan, DM Giles, BN Holben, EJ O'Connor, Y Knyazikhin, and WJ Wiscombe. 2012. "Cloud droplet size and liquid water path retrievals from zenith radiance measurements: examples from the Atmospheric Radiation Measurement Program and the Aerosol Robotic Network." *Atmospheric Chemistry and Physics* 12(21): 10313–10329, https://doi.org/10.5194/acp-12-10313-2012

Chiu, JC, L Gregory, and R Wagener. 2016. MAGIC Cloud Properties from Zenith Radiance Data Final Campaign Summary. U.S. Department of Energy, Atmospheric Radiation Measurement user facility, Richland, Washington. DOE/SC-ARM-15-029.

Cimel (CSPHOT) ARM instrument page: http://www.arm.gov/instruments/csphot

Fairless, T, S Giangrande, C Chiu, L Ma, and R Wagener. 2020. Automated Microphysical Cloud Properties from ARM Cimel Sunphotometer Cloud Mode Datasets. American Geophysical Union, Fall Meeting, abstract #A174-0000.

Holben, BN, TF Eck, I Slutsker, D Tanré, JP Buis, A Setzer, E Vermote, JA Reagan, YJ Kaufman, T Nakajima, F Lavenu, I Jankowiak, and A Smirnov. 1998. "AERONET: A federated instrument network and data archive for aerosol characterization." *Remote Sensing of Environment* 66(1): 1–16, https://doi.org/10.1016/50034-4257(98)00031-5

Mather, JH, and JW Voyles. 2013. "The Arm Climate Research Facility: A Review of Structure and Capabilities." *Bulletin of the American Meteorological Society* 94(3): 377–392, https://doi.org/10.1175/BAMS-D-11-00218.1, 2013

Schaaf, CB, F Gao, AH Strahler, W Lucht, X Li, T Tsang, NC Strugnell, X Zhang, Y Jin, J-P Muller, P Lewis, M Barnsley, P Hobson, M Disney, G Roberts, M Dunderdale, C Doll, RP d'Entremont, B Hu, S Liang, JL Privette, and D Roy. 2002. "First operational BRDF, albedo nadir reflectance products from MODIS." *Remote Sensing of Environment* 83(1-2): 135–148, https://doi.org/10.1016/S0034-4257(02)00091-3

Sookdar, K, SE Giangrande, JD Rausch, L Ma, M Wang, D Wang, MP Jensen, C-S Hung, and JC Chiu. 2025. "Marine and Continental Stratocumulus Cloud Microphysical Properties Obtained from Routine ARM Cimel Sunphotometer Observations." *EGUsphere*, https://doi.org/10.5194/egusphere-2025-694

Stamnes, K, S-C Tsay, WJ Wiscombe, and K Jayaweera. 1988. "Numerically stable algorithm for discrete-ordinate-method radiative transfer in multiple scattering and emitting layered media." *Applied Optics* 27(12): 2502–2509, https://doi.org/10.1364/AO.27.002502

Stephens, GL. 1978. "Radiation profiles in extended water clouds. I: Theory." *Journal of the Atmospheric Sciences* 35(11): 2111–2122, https://doi.org/10.1175/1520-0469(1978)035<2111:RPIEWC>2.0.CO;2

Wang, J, R Wood, MP Jensen, JC Chiu, Y Liu, K Lamer, N Desai, SE Giangrande, DA Knopf, P Kollias, A Laskin, X Liu, C Lu, D Mechem, F Mei, M Starzec, J Tomlinson, Y Wang, S Soo Yum, G Zheng, AC Aiken, EB Azevedo, Y Blanchard, S China, X Dong, F Gallo, S Gao, VP Ghate, S Glienke, L Goldberger, JC Hardin, C Kuang, EP Luke, AA Matthews, MA Miller, R Moffet, M Pekour, B Schmid, AJ Sedlacek, RA Shaw, JE Shilling, A Sullivan, K Suski, DP Veghte, R Weber, M Wyant, J Yeom, M Zawadowicz, and Z Zhang. 2022. "Aerosol and Cloud Experiments in the Eastern North Atlantic (ACE-ENA)." *Bulletin of the American Meteorological Society* 103(2): E619–E641, https://doi.org/10.1175/BAMS-D-19-0220.1

Wood, R, M Wyant, CS Bretherton, J Rémillard, P Kollias, J Fletcher, J Stemmler S de Szoeke, S Yuter, M Miller, D Mechem, G Tselioudis, JC Chiu, JAL Mann, EJ O'Conner, RJ Hogan, X Dong, M Miller, V Ghate, A Jefferson, Q Min, P Minnis, R Palikonda, B Albrecht, E Luke, C Hannay, and Y Lin. 2015. "Clouds, Aerosols, and Precipitation in the Marine Boundary Layer: An Arm Mobile Facility Deployment." *Bulletin of the American Meteorological Society* 96(3): 419–440, https://doi.org/10.1175/BAMS-D-13-00180.1

Appendix A

Input Variables

Tables 1-3 list the various ARM datastreams used in the VAP for data, along with the specific variables in files that are used in processing.

Table 1. Input variables of zenradv3.a1 for SPHOTCOD.

zenradv3.a1 (AEronet Version 3 Zenith Radiance Data)	
Name	**Long Name**
zenith_sky_radiance_A	Sky radiance at zenith (Aureole gain
zenith_sky_radiance_K	Sky radiance at zenith (sky gain)

Table 2. Input variables of modisalbedo.00 for SPHOTCOD.

modisalbedoC1.00 (MODIS Albedo: Extracted from the MODIS "MCD43A3")	
Name	**Long Name**
BRDF_Albedo_Band_Mandatory_Quality_Band1	BRDF_Albedo_Band_Mandatory_Quality_Band1
BRDF_Albedo_Band_Mandatory_Quality_Band2	BRDF_Albedo_Band_Mandatory_Quality_Band2
BRDF_Albedo_Band_Mandatory_Quality_Band3	BRDF_Albedo_Band_Mandatory_Quality_Band3
BRDF_Albedo_Band_Mandatory_Quality_Band4	BRDF_Albedo_Band_Mandatory_Quality_Band4
BRDF_Albedo_Band_Mandatory_Quality_Band5	BRDF_Albedo_Band_Mandatory_Quality_Band5
BRDF_Albedo_Band_Mandatory_Quality_Band6	BRDF_Albedo_Band_Mandatory_Quality_Band6
BRDF_Albedo_Band_Mandatory_Quality_Band7	BRDF_Albedo_Band_Mandatory_Quality_Band7
Albedo_WSA_Band1	Albedo_WSA_Band1
Albedo_WSA_Band2	Albedo_WSA_Band2
Albedo_WSA_Band3	Albedo_WSA_Band3
Albedo_WSA_Band4	Albedo_WSA_Band4
Albedo_WSA_Band5	Albedo_WSA_Band5
Albedo_WSA_Band6	Albedo_WSA_Band6
Albedo_WSA_Band7	Albedo_WSA_Band7

Table 3. Input variables of modisalbedoqc.00 for SPHOTCOD.

modisalbedoC1.00 (MODIS Albedo: Extracted from the MODIS "MCD43A2")	
Name	**Long Name**
BRDF_Albedo_Band_Quality_Band1	BRDF_Albedo_Band_Quality_Band1
BRDF_Albedo_Band_Quality_Band2	BRDF_Albedo_Band_Quality_Band2
BRDF_Albedo_Band_Quality_Band3	BRDF_Albedo_Band_Quality_Band3
BRDF_Albedo_Band_Quality_Band4	BRDF_Albedo_Band_Quality_Band4
BRDF_Albedo_Band_Quality_Band5	BRDF_Albedo_Band_Quality_Band5
BRDF_Albedo_Band_Quality_Band6	BRDF_Albedo_Band_Quality_Band6
BRDF_Albedo_Band_Quality_Band7	BRDF_Albedo_Band_Quality_Band7

Appendix B

Output Variables

Table 4 lists the detailed description of the variables for SPHOTCOD VAP output file. Primary variables are noted in bold.

Table 4. Output variables of the SPHOTCOD VAP.

Name	Long Name	Unit
Time_offset	Time offset from base_time	unitless
Base_time	Base time in Epoch	seconds since 1970-1-1 0:00:00 0:00
time	Time offset from midnight	unitless
time_bounds	Time cell bounds	
gain	Coordinate variable for gain	unitless
modis_channel	Coordinate variable for modis_channel	unitless
modis_wavelength	Central wavelength of modis_channel	nm
modis_white_sky_albedo	Area average of white sky albedo for modis_channel	unitless
aqc_modis_white_sky_albedo	Ancillary quality check results on variable: Area average of white sky albedo for modis_channel	unitless
channel	Coordinate variable for nominal wavelength	unitless
wavelength	Effective Wavelength	um
spectral_irradiance_at_toa	Spectral Irradiance at TOA	W m-2 um-1
solar_zenith_angle	Solar zenith angle	degree
radiance_0440	Normalized zenith radiance at 440nm	unitless
radiance_0870	Normalized zenith radiance at 870nm	unitless
radiance_1640	Normalized zenith radiance at 1640nm	unitless

Name	Long Name	Unit
cloud_optical_depth	**Cloud optical depth**	**unitless**
cloud_optical_depth_std	Standard deviation of cloud optical depth	unitless
liquid_water_path	**Liquid water path**	**g/m2**
liquid_water_path_std	Standard deviation of liquid water path	g/m2
effective_radius	**Effective radius**	**um**
effective_radius_std	Standard deviation of effective radius	um
number_of_solutions	Number of Solutions	count
retrieval_flag	Quality check results	unitless
lat	North latitude	degree_N
lon	East longitude	degree_E
alt	Altitude above mean sea level	m

www.arm.gov

U.S. DEPARTMENT OF ENERGY

Office of Science